HHS Public Access

Author manuscript

Nature. Author manuscript; available in PMC 2019 April 17.

Published in final edited form as:

Nature. 2018 November ; 563(7729): 117–120. doi:10.1038/s41586-018-0636-7.

A mesocortical dopamine circuit enables the cultural transmission of vocal behavior

Masashi Tanaka[1,2], **Fangmiao Sun**[3,4], **Yulong Li**[3,4,5], and **Richard Mooney**[1,*]

[1]Department of Neurobiology, Duke University, Durham, NC 27710 USA

[2]Present Address: Graduate School of Life Sciences, Tohoku University, Sendai, Miyagi 980-8577 Japan

[3]State Key Laboratory of Membrane Biology, Peking University School of Life Sciences, Beijing 100871, China

[4]PKU-IDG/McGovern Institute for Brain Research, Beijing 100871, China

[5]Peking-Tsinghua Center for Life Sciences, Beijing 100871, China

Abstract

The cultural transmission of behavior depends on a pupil's ability to identify and emulate an appropriate tutor[1–4]. How the pupil's brain detects a suitable tutor and encodes the tutor's behavior is largely unknown. Juvenile zebra finches readily copy songs of adult tutors they interact with, but not songs they listen to passively through a speaker[5,6], indicating that social cues generated by the tutor facilitate song imitation. Here we show that neurons in the midbrain periaqueductal gray (PAG) of juvenile finches are selectively excited by a singing tutor and, by releasing dopamine (DA) in a sensorimotor cortical analogue (HVC), help encode tutor song representations used for vocal copying. Blocking DA signaling in the pupil's HVC during tutoring blocked copying, whereas pairing stimulation of PAG terminals in HVC with song played through a speaker was sufficient to drive copying. Exposure to a singing tutor triggered the rapid emergence of responses to the tutor song in the pupil's HVC and a rapid increase in the pupil's song complexity, an early signature of song copying[7,8]. These findings reveal that a dopaminergic mesocortical circuit detects a tutor's presence and helps encode the tutor's performance, facilitating the cultural transmission of vocal behavior.

The cortical song nucleus HVC is crucial to singing and song learning[7,9–12] and receives convergent input from premotor, auditory, and neuromodulatory afferents, including

[*]**Correspondence and requests for materials** should be addressed to R.M. mooney@neuro.duke.edu.

Author contributions

M.T. and R.M. designed experiments. F.S. and Y.L. developed DA sensors, M.T. performed experiments and analyzed data. M.T. and R.M. wrote the manuscript.

Data availability

The datasets generated and analyzed during the current study are available from the corresponding author on reasonable request.

Competing interests

F.S. and Y.L. have filed patent applications whose value might be affected by this publication.

dopamine (DA)-secreting neurons in the midbrain periaqueductal gray (PAG)[13–15] (Fig. 1a-c, Extended Data Fig. 1a-c). In the mammalian PAG, DA neurons encode information about social context, arousal in response to behaviorally salient stimuli, or reward[16–18], raising the possibility that the PAG to HVC pathway in juvenile finches encodes information about the tutor that facilitates song imitation. To explore this idea, we implanted tetrodes into the PAG of juvenile male finches raised in isolation from a tutor (tutor-naive juveniles; see Methods) (Fig. 1d-k). Most PAG neurons (81.8%: 18/22 neurons from 4 birds) increased their action potential activity in the presence of a singing tutor (Fig. 1e-g, k), whereas PAG activity was unaffected during encounters with non-singing adult male finches or female finches, which do not sing (Fig. 1i-j, k). Neural activity in the juvenile's PAG was not precisely locked to syllables of the tutor song, was variable across different tutor song bouts, and could remain elevated for hundreds of milliseconds after the tutor stopped singing (Extended Data Fig. 2c-f), suggesting that PAG activity evoked by a singing tutor is not simply auditory in nature. Indeed, playback of adult finch song from a speaker, including that of a recent tutor, failed to evoke activity in the juvenile's PAG (Fig. 1h, k). Moreover, song playback from a speaker in the presence of an adult female bird failed to activate PAG neurons in tutor-naive juveniles (Extended Data Fig. 2a,b). Therefore, PAG neurons in juvenile males respond strongly and selectively to a live singing tutor and thus can signal the presence of a suitable song model.

These findings raise the possibility that experience of a singing tutor stimulates DA release from PAG terminals in HVC. We explored this idea by virally expressing a modified dopamine type 2 (D2) receptor in HVC neurons of tutor-naive juvenile males that increases fluorescence upon DA binding (Fig. 2) (AAV 2/9 $GRAB_{DA1h}$)[19]. We then head-fixed these juvenile males in the awake state and used two-photon imaging methods[20] to establish that DA levels in HVC increase in the presence of a singing tutor (Fig. 2c-d, i). In contrast, DA-related changes in fluorescence were not detected in the juvenile's HVC in response to song playback (Fig. 2e, i), or when the juvenile encountered non-singing adult males or females (Fig. 2f, g, i), paralleling the selective enhancement of PAG activity elicited by a singing tutor. Moreover, ablating DA neurons in the pupil's PAG with 6-hydroxydopamine (6-OHDA[21]) prevented tutor-evoked DA transients in the pupil's HVC (Fig. 2h, i), confirming that tutor-evoked DA release in the pupil's HVC largely originates from the PAG

To explore whether DA signaling in HVC plays a role in song imitation, we used 6-OHDA to lesion DA-releasing fibers in the HVC of juvenile male finches raised continuously with adult male tutors and tracked their song development into adulthood (Fig. 3a-c, Extended Data Fig. 3). Lesions of DA-releasing fibers in HVC made near the onset of the sensitive period for tutor song memorization (30 days-post-hatch[22] or 30 d) prevented song copying (Fig. 3d-e) without affecting the overall rate of singing (Extended Data Fig. 4a). As adults, these 6-OHDA treated birds produced abnormally long and acoustically simple syllables, similar to finches raised in isolation from a tutor[22] (Extended Data Fig. 4b, c). The 6-OHDA lesions made in HVC in 30 d males are permanent and thus could potentially interfere with tutor song memorization (i.e., sensory learning), the subsequent phase of song copying (sensorimotor learning), or both. However, 6-OHDA lesions made in the HVC of 45 d males, which have had sufficient tutor experience to enable accurate copying but are just beginning sensorimotor learning[22], did not affect the juvenile's ability to copy a tutor song (Fig. 3d, f).

These findings suggest that DA signaling in HVC plays a role in sensory learning but cannot exclude a more general but developmentally restricted (before 45d, e.g.) role for such signaling. Therefore, we used microdialysis methods[23] to reversibly block DA receptors in the HVC[24] of tutor-naive juvenile males (Age: 43.0 ± 4.9 d [mean ± SD], $n = 5$) while they were housed with a tutor for 1.5 h on five consecutive days, allowing us to better determine whether DA signaling in HVC is crucial during pupil-tutor interactions, when sensory learning occurs (Fig. 3g-h, Extended Data Fig. 5a-c). Reversibly blocking DA receptors in HVC during but not just after tutoring sessions blocked song copying (Fig. 3h, Extended Data Fig. 5b-c), without affecting juveniles' attentive behaviors to tutors or tutors' singing rates (Extended Data Fig. 5d-e, Supplementary Video 1–2). Moreover, reversibly suppressing PAG activity in the pupil with muscimol during daily tutoring sessions also blocked song copying; notably, juveniles in which PAG was inactivated also failed to orient to their tutors, even though tutors continued singing at normal rates (Extended Data Fig. 5d-h, Supplementary Video 3). Thus, tutor-evoked activation of the pupil's PAG and concomitant release of DA in HVC are essential to encoding tutor song experience, and PAG activity may be required for the pupil to attend to a singing tutor.

The current findings do not exclude the possibility that DA signaling at other sites also contributes to sensory learning. One potential site is the basal ganglia region Area X[11], which receives dopaminergic input from the ventral tegmental area and substantia nigra pars compacta (VTA/SNc), as well as from a smaller cohort of TH+ PAG neurons (Extended Data Fig. 1d-g), and where dopamine signaling plays a role in sensorimotor learning[25]. Nonetheless, infusing DA receptor blockers into Area X of juvenile males during daily tutoring sessions did not affect song copying (Extended Data Fig. 6). Another potential site is the caudal mesopallium (CM), an auditory forebrain region important to song memory[26,27]. However, blocking DA receptors in the CM of juvenile males during daily tutoring sessions did not block song copying (Extended Data Fig. 5i-k).

These results show that DA release from PAG axon terminals in HVC (PAG_{HVC} terminals) signals the presence of a suitable model and helps encode this model in the pupil's brain. Consequently, artificially activating PAG_{HVC} terminals should compensate for the absence of a live tutor and facilitate vocal copying in response to song playback. To test this idea, we used AAVs to express channelrhodopsin-2 (ChR2) bilaterally in the PAG of tutor-naive juvenile males (Fig. 3i-j, Extended Data Fig. 7a-d). Several weeks (33.3 ± 7.4 days [mean ± SD], $n = 6$) later, we implanted optical fibers bilaterally over HVC and optogenetically activated PAG_{HVC} terminals while playing an adult male zebra finch song through a speaker. Pairing PAG_{HVC} terminal stimulation with song playback resulted in a significant level of song copying compared to juveniles that had only been exposed to song playback, or to song playback and optical illumination of HVC in the absence of ChR2 (Fig. 3j, Extended Data Fig. 7b; see Methods). Moreover, pairing song playback with PAG_{HVC} terminal stimulation while infusing DA blockers into HVC did not lead to song copying in tutor-naive juveniles (Extended Data Fig. 7e-g).

To explore how tutor-evoked DA release from PAG_{HVC} axon terminals alters HVC to drive song imitation, we implanted tetrodes in the HVC of tutor-naive juveniles and recorded neural activity before and after their initial encounters with a singing tutor (Fig. 4a-f).

Spontaneous burst firing in HVC neurons increased within 1 h after the juvenile's initial exposure to a singing tutor (Fig. 4b-c, e), without any change in their mean firing rates (Extended Data Fig. 8d). Because burst firing in HVC is driven by auditory afferents[12], this enhanced bursting suggests that tutoring rapidly potentiates auditory inputs to HVC. In fact, brief (35.0 ± 16.8 min [mean ± SD]) experience with a singing tutor led rapidly (~1 h) to the emergence of temporally precise responses in the awake juvenile HVC to tutor song playback (Fig. 4d, f, Extended Data Fig. 8a-c). Furthermore, the mean firing rate of HVC neurons to song playback was unaffected by tutoring (Extended Data Fig. 8e-f), indicating that neural responses in HVC became more tightly locked to specific features in the tutor song. None of these juveniles (n = 4) sang during or for several hours after the tutoring session, and thus these physiological changes were not simply the result of auditory feedback associated with vocal rehearsal. In another set of tutor-naive juvenile males, we found that tutoring rapidly reduced the kurtosis of vocal duration (Fig. 4g-h) and increased the mean entropy variance of the juveniles' songs (Fig. 4i), two early hallmarks of song copying[7,8]. Notably, blocking DA signaling in the pupil's HVC with 6-OHDA or DA blockers prevented these physiological and behavioral changes (Fig. 4e, f, h-i).

The discovery that DA neurons in the pupil's PAG are strongly and selectively activated by a singing tutor parallels an emerging body of evidence that potentially homologous neurons in the mammal can encode social cues, including those related to reward, context, or novelty[16,17]. Indeed, the present findings advance a model in which both social cues and the song-related auditory input provided by the singing tutor drive the coincident activation of DA receptors and auditory synapses in HVC, leading to the rapid emergence of auditory representations of the tutor's song necessary to song imitation[10,20] (Extended Data Fig. 10). This coincident encoding mechanism could help ensure that the pupil's brain selectively forms representations of songs produced by suitable adult tutors, and not of extraneous auditory stimuli. Although DA-dependent modulation of auditory cortical representations has previously been linked to perceptual learning[28], a notable feature of the DA-dependent process of auditory encoding described here is that it occurs in a vocal motor region and rapidly drives vocal imitation. More broadly, DA signaling is enhanced in the motor cortex of primates relative to other mammals[29,30], raising the possibility that augmented DA signaling in motor regions of songbirds and primates reflects a convergent neural architecture for promoting motor imitation in response to social models.

Methods

Animal model

Juvenile male (15–90 d), adult male (>200 d), and adult female (>200 d) zebra finches (*Taeniopygia guttata*) were obtained from the Duke University Medical Center breeding facility. All experimental procedures were in accordance with the NIH guidelines and approved by the Duke University Medical Center Animal Care and Use Committee. Birds were kept under a 14/10-h light/dark cycle with free access to food and water. Data were collected from 96 birds (Supplementary Table).

Song analysis

Songs were automatically recorded with Sound Analysis Pro (SAP2011)[31] in a soundproof box. Vocalizations of >10 ms were detected by thresholding of the recorded sounds. Imitation of the tutor song was quantified as percent similarity (asymmetrical similarity) between the song motifs from pupil birds and their tutors using SAP2011[31] with default parameters for zebra finches, and reported as tutor song similarity. First, the song motif (a stereotyped sequence of syllables constituting an adult zebra finch song) of each bird was determined as the most frequently observed syllable sequence. Then, percent similarity was calculated for representative song motifs randomly chosen from pupils and their tutor, and averaged across ≥10 comparisons to report as tutor song similarity. For immature subsongs that do not have a stereotyped song motif, we used randomly chosen part of subsongs with the duration similar to the tutor song motif for calculating percent similarity. For isolated birds in Extended Data Fig. 4c, percent similarity was calculated between the song motifs from isolated birds and unrelated, normally raised adult zebra finches. A song bout was detected as successive vocalizations with ≥3 syllables (to exclude call bouts) separated by an inter-bout interval of >400 ms. Kurtosis of vocal duration and Wiener entropy variance (EV) were calculated based on all the song bouts in each 90-minute time window.

Tutoring of juvenile birds

Juvenile birds were raised by their parents with their siblings until ~45 d in experiments depicted in Fig. 3a-f. Otherwise, juvenile birds were separated from their parents and siblings at 15–30 d (i.e., tutor-naive juveniles), and encountered an unfamiliar adult male (tutor) only during tutoring sessions. During a tutoring session, a juvenile bird and tutor were separated by a plastic grating or transparent glass, so they could acoustically and visually interact but direct physical interactions were prevented. The tutor was either manually introduced into the neighboring chamber by an experimenter, or presented through an electric glass whose transparency can be remotely controlled. Attention of juvenile birds to the tutor was quantified as the time that juvenile birds were awake and near the tutor without foraging, drinking, preening, or singing, and normalized to the total time of observation (>5 min) during tutoring sessions. Untutored isolated birds depicted in Extended Data Fig. 4b-c were kept isolated from adult males until 90 d.

General surgery

Detailed procedures of surgery were previously provided[23]. Briefly, juvenile birds were anesthetized with 2% isoflurane inhalation and placed on a custom stereotaxic apparatus with a heat blanket. Target cites for injection and implantation were determined by stereotaxic coordinates and multiunit activity. Stereotaxic coordinates were [0.0 mm rostoral, 2.4 mm lateral, and 0.5 mm ventral] for HVC; [3.4 mm rostral, 0.5 mm lateral, and 6.3 mm ventral (head angle: 58°)] for PAG; [5.8 mm rostral, 1.6 mm lateral, and 3.0 mm ventral (head angle: 40°)] for Area X; and [1.3 mm rostral, 1.2 mm lateral, and 0.5 mm ventral] for CM. Reagents or viruses were injected using Nanoject-II (Drummond Scientific). Viral injection was performed bilaterally with the volume of 483–966 nL per hemisphere. Viruses were obtained from the Penn Vector Core (Pennsylvania, USA), UNC Vector Core (Chapel Hill, USA), Janelia Virus Service Facility (Ashburn, USA), and Vigene

Biosciences (Rockville, USA). Experiments were performed >30 d after the viral injection. Birds with unsuccessful injection or implantation were discarded from the analysis.

Injection of 6-OHDA

Juvenile birds received bilateral injection of 200–450 nL 6-OHDA solution into HVC at either ~30 d (mean ± SD: 30.1 ± 4.2 d, range: 25–34 d, $n = 7$) or ~45 d (mean ± SD: 44.5 ± 3.0 d, range: 39–47 d, $n = 6$). The solution was PBS-based and included 5–20 mM 6-OHDA hydrochloride (Santa Cruz, sc-203482), 10 mM L-ascorbic acid (MilliporeSigma, A92902), and 1 μM desipramine hydrochloride (Tocris, 3067), which was included as an inhibitor for noradrenaline and serotonin transporters to protect noradrenergic and serotonergic neurons at the injection site. Control birds received injection of PBS with 10 mM ascorbic acid and 1 μM desipramine at ~30 d (mean ± SD: 29.3 ± 3.6 d, range: 22–32 d, $n = 7$). Drugs were dissolved into PBS immediately before injection in place of equimolar NaCl (Working solution: ~300 mOsm, pH 7.3). After injection, birds were returned to their original home cage until ~45 d when they were isolated in a soundproof box until 90 d.

Microdialysis infusion of drugs

Tutor-naive juveniles (~45 d, mean ± SD: 43.8 ± 5.5 d, range: 32–57 d, $n = 34$) received bilateral implantation of a microdialysis probe. After 1–3 d of implantation (mean ± SD: 45.5 ± 5.8 d, range: 33–60 d, $n = 34$), tutoring sessions were conducted for 5 consecutive days. Each tutoring session consisted of 90-minute tutor presentation. Drug was infused into the target area (HVC, Area X, CM, or PAG) either 90 minutes before or immediately after the tutor presentation, and washed with saline 180 minutes after the injection (Fig. 3g). The tutor bird typically sang >30 motifs in a session (See Extended Data Fig. 5e). For a session in which the tutor did not sing any song, an additional tutoring session was conducted on the next day. As a blocker for D1- and D2-type receptors, 5 mM R(+)-SCH-23390 hydrochloride (MilliporeSigma, D054) and 5 mM S-(−)-sulpiride (Tocris, 0895) were respectively used and dissolved into saline. To inactivate PAG, 2.5 mM muscimol (MilliporeSigma, M-1523) dissolved into saline was infused into the PAG.

Histology and imaging

Birds were deeply anesthetized with intramuscular injection of 20 μL Euthasol (Virbac) and transcardially perfused with PBS, followed by perfusion with 4% (wt/vol) paraformaldehyde (PFA) in PBS. The removed brain was post-fixed and cryoprotected with 30% (wt/vol) sucrose and 4% (wt/vol) PFA in PBS overnight. Frozen sagittal sections (thickness of 50 μm) were prepared with a sledge microtome (Reichert) and collected in PBS. For immunohistochemistry, sections were washed twice in PBS, permeabilized with 0.3% Triton X-100 in PBS (PBST) for 1 h, blocked with 10% Blocking One Histo (06349–64, Nacalai Tesque) in PBST for 1 h, and incubated with rabbit primary antibody for TH (1:500, AB152; MilliporeSigma) or rabbit primary antibody for DBH (1:2000, #22806; ImmunoStar) in PBST with 10% Blocking One Histo at 4 °C overnight. Then, sections were washed three times in PBST and incubated with anti-rabbit secondary antibody (1:500; Jackson ImmunoResearch) in PBST at room temperature for 1 h, followed by three washes in PBS. Sections were coverslipped with Fluoromount-G (SouthernBiotech), and then imaged with a confocal microscope (SP8; Leica) through a 20x objective lens controlled by LAS X

software (Leica). To label PAG neurons that project to HVC or Area X, dextran Alexa Fluor 488 (D-22910; ThermoFisher) was injected into HVC or Area X of juvenile birds (Age: mean ± SD: 35.3 ± 7.0 d, range: 28–42 d, $n = 3$ for HVC, Age: mean ± SD: 47.7 ± 15.3 d, range: 36–65 d, $n = 3$ for Area X) 4–7 d before perfusion. Retrogradely labeled neurons were manually counted in PAG and SNc/VTA, each of which was densely packed with TH-positive (TH+) neurons. Images were shown as max-projected images of sagittal sections. To quantify TH+ fibers in HVC, TH+ fibers in HVC shelf/NCL, and DBH+ fibers in HVC, the fiber density was calculated in >0.04 mm^2 areas from each region as the fraction of areas with the fluorescence more than [mean + 10 SD] of the background fluorescence. For analysis on HVC shelf/NCL, a >0.04 mm^2 region located ~0.6 mm ventral from HVC was manually selected.

Two-photon imaging and analysis:

Viruses coding DA sensors (AAV2/9-hSyn-$GRAB_{DA1h}$ or AAV2/9-CAG-$GRAB_{DA1h}$), developed in Yulong Li's lab[19], were injected into HVC of tutor-naive juveniles (~30 d, mean ± SD: 32.6 ± 5.3 d, range: 25–39 d, $n = 5$), and HVC was imaged after implantation of a head-post and cranial window >30 days later (mean ± SD: 66.6 ± 6.0 d, range: 60–73 d, $n = 5$). To ablate DA-releasing PAG neurons, 200 nL 6-OHDA solution (10 mM 6-OHDA, 10 mM L-ascorbic acid, and 1 μM desipramine hydrochloride) was injected into PAG 2 days before imaging. Images were collected at 15.5 Hz with a resonant scanning two-photon microscope (Neurolabware) that applies a mode-locked titanium sapphire laser (Mai Tai DeepSee) at 920 nm through a 16x objective lens (0.8 NA water immersion, Nikon). The objective lens was covered with black cloth to prevent room light from being detected by the photomultipliers. During imaging, a head-fixed bird in a dim room experienced playback of an adult zebra finch (tutor) song bout (3 seconds. 7 introductory notes and 3 motifs comprising 5 syllables), encounters with an adult male tutor, encounters with an adult female bird, and a singing tutor with a randomized order. Images were acquired >10 trials for each condition, and regions of interest (ROIs) were automatically or manually selected after image alignment with MATLAB programs (Scanbox). After subtraction of background fluorescence in an annular region surrounding each ROI, signals were calculated as mean fluorescence within each ROI. Then, $\Delta F/F$ of the ROI was calculated for each trial as 100 * $(F(t) - F_0) / F_0$ [%], where $F(t)$ was a time series of ROI signals, and F_0 was the average of baseline ROI signals for the 5 s-period just before the onset of stimulus presentation. Mean $\Delta F/F$ was calculated for the 5 s-period after the onset of stimulus presentation, and averaged across trials in each condition.

Optogenetics

Tutor-naive juvenile birds received injection of either AAV2/9-CAG-ChR2-mCherry, AAV2/1-CAG-ChR2-mCherry, or AAV2/9-CAG-NRX-ChR2-YFP to PAG at ~35 d (mean ± SD: 34.0 ± 4.8 d, range: 30–40 d, $n = 9$). Laser was bilaterally applied through optic fibers (core: 200 μm; Thorlabs) implanted to HVC. Juvenile birds received a tutoring session per day for 5 consecutive days starting at ~60–70 d (mean ± SD: 64.0 ± 4.9 d, range: 61–71 d, $n = 9$). In each tutoring session, a juvenile bird experienced playback of a song bout (mean amplitude: 70 dB SPL, 7 introductory notes and 3 motifs comprising 5 syllables) 10 times (30 motifs) within 30 minutes. To block DA signaling in HVC, DA blockers were infused

into HVC with microdialysis probes 90 minutes before the tutoring session, and washed with saline immediately after the tutoring session ($n = 3$). Experimental birds received repetitive laser stimulation (10 ms; 20 Hz) throughout the playback. Control birds consisted of a group that received injection of viruses coding GFP and implantation of optic fibers ($n = 2$, scAAV2/9-CMV-GFP or AAV2/9-CAG-GFP) at ~35 d (mean ± SD: 36.5 ± 6.4 d, range: 32–41 d, $n = 2$), a group that did not receive viral injection but implantation of optic fibers ($n = 2$), and a group that did not receive injection, implantation, or laser stimulation ($n = 2$). These groups listened to playback in the same way as experimental birds (Age: mean ± SD: 58.5 ± 8.5 d, range: 54–73 d, $n = 6$), and were analyzed together since we did not find significant differences in learning abilities between these groups.

Chronic recording from PAG and HVC

Tetrodes (A2×2-tet-3/10mm-150–150-121, NeuroNexus) were implanted into the HVC or the PAG of tutor-naive juveniles (Age: mean ± SD: 51.3 ± 13.4 d, range: 27–71 d, $n = 11$). Birds were habituated to a dummy probe (1.5–2 g) on the head for ~7 d before the implantation. Data were collected with a universal serial bus (USB) interface board (RHD2000; Intan Technologies) after band-pass filtering (0.2–10 kHz) and sampling at 30 kHz with a small amplifier board (RHD2132 16-Channel; Intan Technologies) on the bird's head. Unit activity was sorted in a semi-automated fashion with a custom C++ software using a support vector machine algorithm (M.T.). Unit activity with a mean amplitude >3 SD of noise was used for subsequent analysis. Recording of song-related activity was triggered by xpctarget in MATLAB (MathWorks). To block DA signaling in HVC, juvenile birds received an injection of 6-OHDA into HVC 2–5 days before tetrode recording from the same HVC. Mean FR of PAG neurons was calculated for >10 trials with >0.5 seconds after the onset of singing or song playback and 5 s after presentation of a male or female bird, and averaged after normalization with mean spontaneous FR calculated for >10 seconds before the presentation of stimuli. Probability of burst activity in HVC neurons was calculated for >300 s spontaneous activity before and after exposure to a live tutor. CV FR across trials of HVC neurons was calculated for 50 ms-bin with a hop size 1 ms across >15 trials, and reported as average of CV FR from all the bins in the motif (>0.5 seconds) if the mean FR during playback was >0.05 Hz. For data analysis, Igor Pro (WaveMetrics), MATLAB, and Microsoft Excel were used.

Statistics

Error bars and values in the text indicate mean ± standard error of mean (SEM), unless otherwise noted. Two-way ANOVA was performed in MATLAB to examine significance of the main effect of 6-OHDA ($F(2,85) = 53.10$, $P < 0.001$) (Fig. 3e-f), DA blockers to HVC, DA blockers to CM, and muscimol to PAG ($F(5,99) = 23.17$, $P < 0.001$) (Fig. 3h and Extended Data Fig. 5c, h, k), DA blockers to Area X ($F(1,30) = 0.22$, $P = 0.640$) (Extended Data Fig. 6c), optogenetic activation of PAG terminals in HVC ($F(2,47) = 16.61$, $P < 0.001$) (Fig. 3j and Extended Data Fig. 7f), followed by post-hoc Tukey-Kramer test to report significant difference between conditions at each age window. To examine the different proportion of labeled neurons in PAG and VTA/SNc, χ^2-tests were performed. Two-way ANOVA was performed in MATLAB to examine significance of the main effect of blockage of DA signaling on kurtosis syllable duration ($F(1,39) = 19.69$, $P < 0.001$) (Fig. 4h), entropy

variance ($F(1,39) = 4.84$, $P = 0.034$) (Fig. 4i), and song rate ($F(1,39) = 0.16$, $P = 0.691$) (Extended Data Fig. 9), followed by Tukey-Kramer test to report significant difference between conditions at each time window, and by paired *t*-test with Bonferroni correction to report significant difference between before and after exposure to tutor songs. One-way ANOVA was performed in MATLAB to examine the main effect of different conditions in Fig. 1k and Extended Data Fig. 2b ($F(4,93) = 6.84$, $P < 0.001$), Fig. 2i ($F(4,23) = 10.31$, $P < 0.001$), Extended Data Fig. 3c ($F(2,12) = 13.42$, $P < 0.001$), Extended Data Fig. 3d ($F(2,12) = 0.14$, $P = 0.870$), Extended Data Fig. 4a ($F(2,17) = 0.28$, $P = 0.757$), Extended Data Fig. 5d ($F(2,7) = 30.40$, $P < 0.001$), and Extended Data Fig. 5e ($F(2,10) = 0.78$, $P = 0.486$), each followed by Tukey-Kramer test to report significant difference between conditions. In other analyses, paired *t*-test (Figs. 1k, 2i, 4h,i, Extended Data Figs. 2b, 8d-f) or unpaired *t*-tests (Extended Data Figs. 3e, 4c) were performed in Microsoft Excel. Multiple data from a bird are indicated with the same markers in Figs. 1c,g,k, 2i, 4e,f and Extended Data Figs. 1b,c,e,f,g, 2b, 3c-e, 8d-f. Statistical tests performed were two-sided. Asterisks show $P < 0.050$.

Code availability:

Custom code or software is available from the corresponding author upon reasonable request.

Extended Data

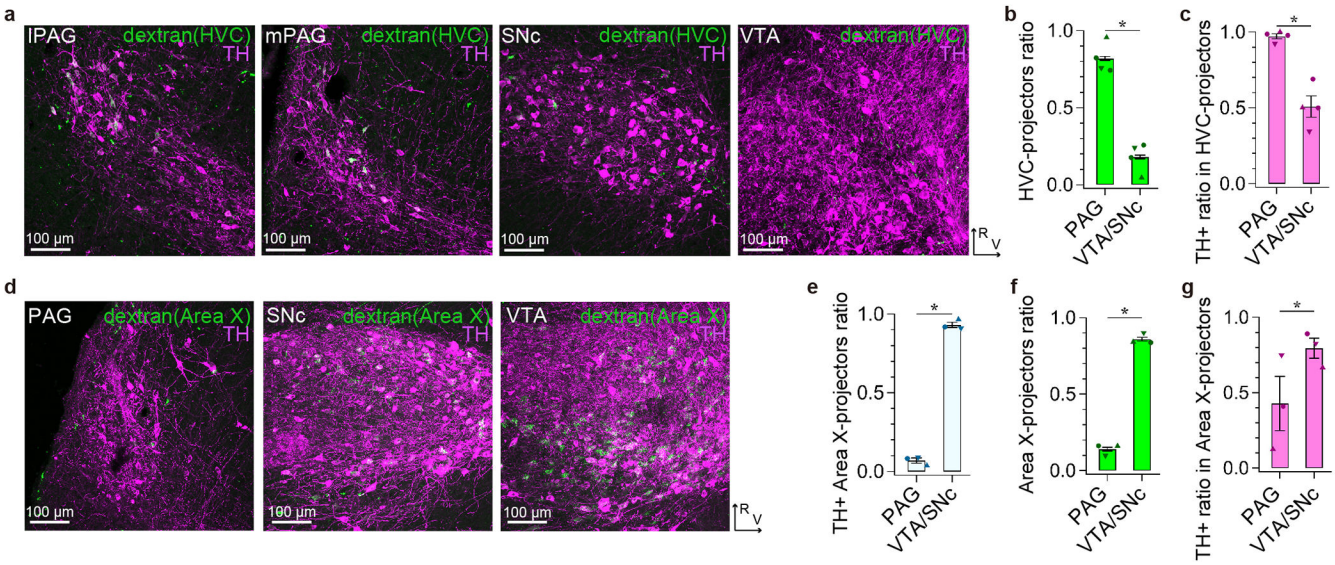

Extended Data Figure 1 |. Distribution of HVC-projecting neurons and Area X-projecting neurons in the midbrain.

a, From left to right, a max-projected image of serial sagittal sections visualized with a confocal microscope, showing a lateral part of PAG (lPAG) (~1.0 mm lateral), a medial part of PAG (mPAG, ~0.2 mm lateral), SNc (~1.2 mm lateral), and VTA (~0.2 mm lateral), each of which was labeled with dextran injected into HVC (green) and an antibody for TH (pseudo-colored magenta). Similar results were obtained in 4 independently repeated experiments (R: rostral, V: ventral). **b**, Proportion of HVC-projecting neurons in PAG and

VTA/SNc (χ^2-test: $\chi^2(1) = 406.54$, $P < 0.001$, $n = 4$ hemispheres from 3 birds). **c**, Proportion of TH-positive (TH+) neurons in HVC-projecting neuron subsets in PAG and VTA/SNc (χ^2-test: $\chi^2(1) = 204.62$, $P < 0.001$, $n = 4$ hemispheres from 3 birds). **d**, From left to right, a max-projected image of serial sagittal sections visualized with a confocal microscope, showing PAG (~0.6 mm lateral), SNc (~0.6 mm lateral), and VTA (~0.2 mm lateral), each of which was labeled with dextran injected into Area X (green) and an antibody for TH (pseudo-colored magenta). Similar results were obtained in 3 independently repeated experiments. **e**, Proportion of double-labeled neurons (dextran and TH) in PAG and SNc/VTA (χ^2-test: $\chi^2(1) = 493.92$, $P < 0.001$, $n = 3$ hemispheres from 3 birds) in birds that received injection of dextran into Area X. **f**, Proportion of Area X-projecting neurons in PAG and VTA/SNc (χ^2-test: $\chi^2(1) = 472.07$, $P < 0.001$, $n = 3$ hemispheres from 3 birds). **g**, Proportion of TH+ neurons in Area X-projecting neuron subsets in PAG and VTA/SNc (χ^2-test: $\chi^2(1) = 55.14$, $P < 0.001$, $n = 3$ hemispheres from 3 birds). Error bars indicate mean ± SEM.

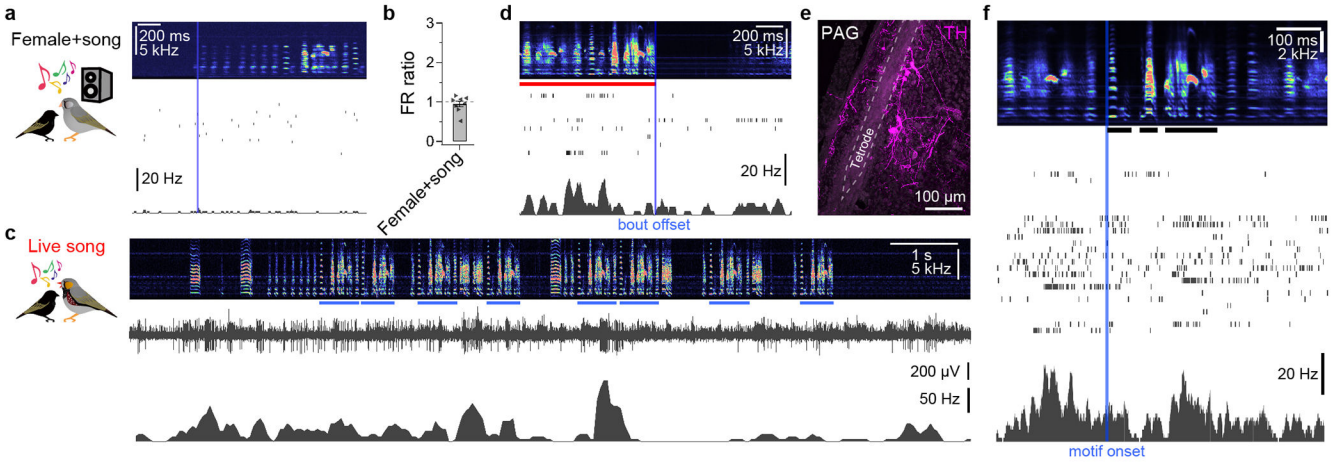

Extended Data Figure 2 |. Juvenile male PAG activity in response to song playback in the presence of a female bird and live songs of a male bird.

a, Tutor-naive juvenile male finch PAG activity aligned to the onset of 35 presentations of song playback in the presence of an adult female bird (top: averaged sound spectrogram, middle: spike raster plot, bottom: mean firing rate). **b**, Mean firing rate (FR) during presentation of song playback in the presence of a female bird, normalized to baseline FR (two-sided paired *t*-test: $t(7) = 0.620$, $P = 0.555$; $n = 8$ neurons from 2 birds). **c**, PAG activity during a tutor song bout (top: sound spectrogram, middle: voltage recording, bottom: firing rate, blue bar: song motif). **d**, PAG unit activity aligned to the offset of a live tutor's song bouts (red bar: live song), shown as in **a**. **e**, A max-projected image of serial sagittal sections visualized with a confocal microscope, showing the site of tetrode recordings in PAG (~0.8 mm lateral of the midline). **f**, PAG unit activity aligned to the onset of live tutor's song motifs, shown as in **a**. Note that the tutor often sings multiple motifs within a single bout, thus some motifs precede (and follow) the alignment time. Error bars indicate mean ± SEM.

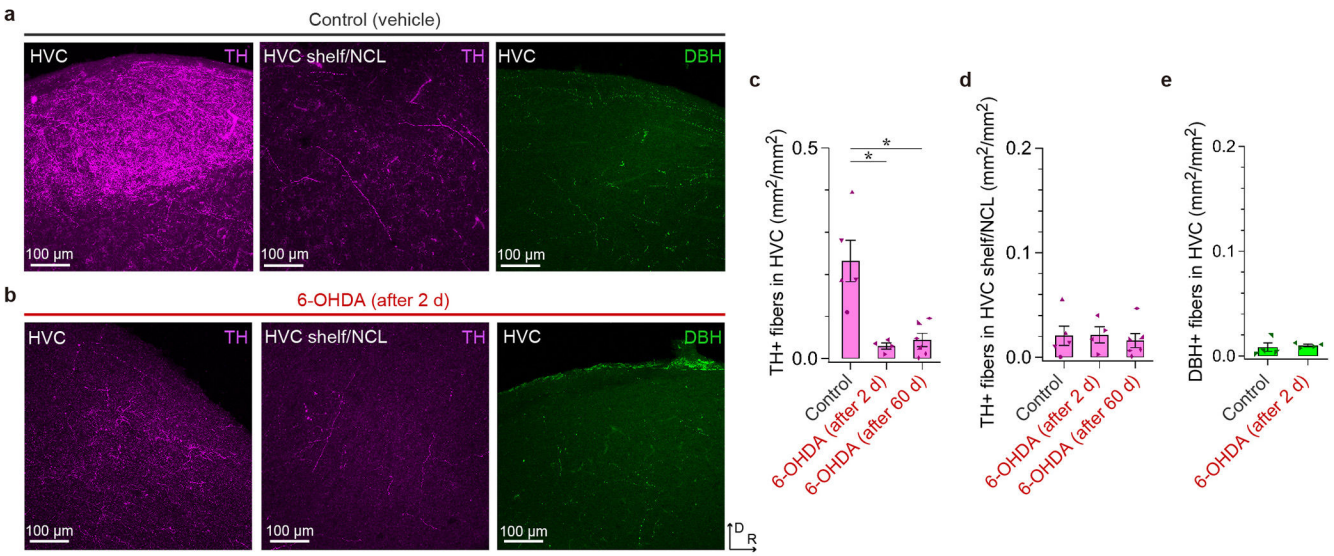

Extended Data Figure 3 |. Effects of 6-OHDA injection into HVC on DA fibers in HVC and surrounding regions and on noradrenergic/adrenergic fibers in HVC

a, From left to right, a max-projected image of serial sagittal sections visualized with a confocal microscope, showing HVC with TH immunolabeling (~2.4 mm lateral), HVC shelf and caudolateral nidopallium (NCL) just ventral to HVC with TH immunolabeling (~2.4 mm lateral), and HVC with dopamine beta-hydroxylase (DBH) immunolabeling (~2.4 mm lateral) in control birds, which received injection of vehicle into HVC. Similar results were obtained in 5 independently repeated experiments (orientation is similar to **b**). **b**, From left to right, a max-projected image of serial sagittal sections visualized with a confocal microscope, showing HVC with TH immunolabeling (~2.4 mm lateral), HVC shelf and NCL just ventral to HVC with TH immunolabeling (~2.4 mm lateral), and HVC with DBH immunolabeling (~2.4 mm lateral) in birds that received injection of 6-OHDA into HVC 2 days before tissue fixation. Similar results were obtained in 4 independently repeated experiments (D: dorsal, R: rostral). **c**, Density of TH-positive (TH+) fibers in HVC of control birds (n = 5 hemispheres from 3 birds) was higher than that of birds that received injections of 6-OHDA 2 days before fixation (Tukey-Kramer test: P = 0.002) (n = 4 hemispheres from 2 birds), and that of birds that received injections of 6-OHDA ~60 days before fixation, as in Fig. 3b-c (Tukey-Kramer test: P = 0.002) (n = 6 hemispheres from 4 birds). **d**, Density of TH+ fibers in HVC shelf and NCL in control birds (n = 5 hemispheres from 3 birds), birds that received injection of 6-OHDA 2 days before fixation (n = 4 hemispheres from 2 birds), and birds that received injection of 6-OHDA ~60 days before fixation, as in Fig. 3b-c (n = 6 hemispheres from 4 birds). **e**, Density of DBH-positive (DBH +) fibers in HVC in control birds (n = 4 hemispheres from 2 birds) and birds that received injection of 6-OHDA 2 days before injection (n = 4 hemispheres from 2 birds) was not significantly different (two-sided unpaired t-test: $t(7)$ = 0.379, P = 0.716). Error bars indicate mean ± SEM.

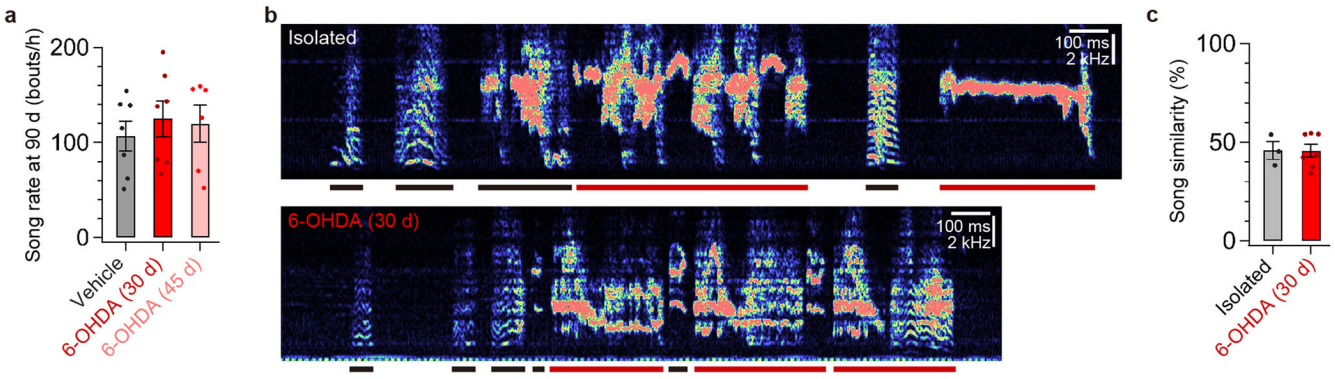

Extended Data Figure 4 |. Ablation of DA terminals in HVC did not affect song rate but decreased song imitation to the level of birds raised in isolation from a tutor.

a, The song rates of birds that received injection of vehicle ($n = 7$), 6-OHDA at ~30 d ($n = 7$), and 6-OHDA at ~45 d ($n = 6$) were not significantly different (one-way ANOVA: $F(2,17) = 0.283$, $P = 0.757$). **b**, Spectrograms from a 90-d bird that was raised in isolation from a tutor (top) and from a 90-d bird that was normally tutored but received injection of 6-OHDA into HVC at 30 d (bottom). **c**, Similarity of 90-d untutored (Isolated) birds' songs to songs of unrelated adult zebra finches that had been normally tutored ($n = 3$) was not significantly different from tutor song similarity of 90-d pupils that received injection of 6-OHDA into HVC at ~30 d ($n = 7$) (two-sided unpaired t-test: $t(9) = 0.013$, $P = 0.990$), but was significantly different from tutor song similarity of 90-d pupils that received injection of vehicle at ~30 d ($n = 7$) ($t(9) = 3.028$, $P = 0.014$), or from tutor song similarity of 90-d pupils that received injection of 6-OHDA into HVC at ~45 d ($n = 6$) (two-sided unpaired t-test: $t(8) = 3.314$, $P = 0.011$) (song data from birds injected with 6-OHDA into HVC at ~30 d is same as Fig. 3e; song similarity data from birds injected in HVC with vehicle at ~30 d or 6-OHDA at ~45 d are not shown here but are shown in Fig. 3f). Error bars indicate mean ± SEM.

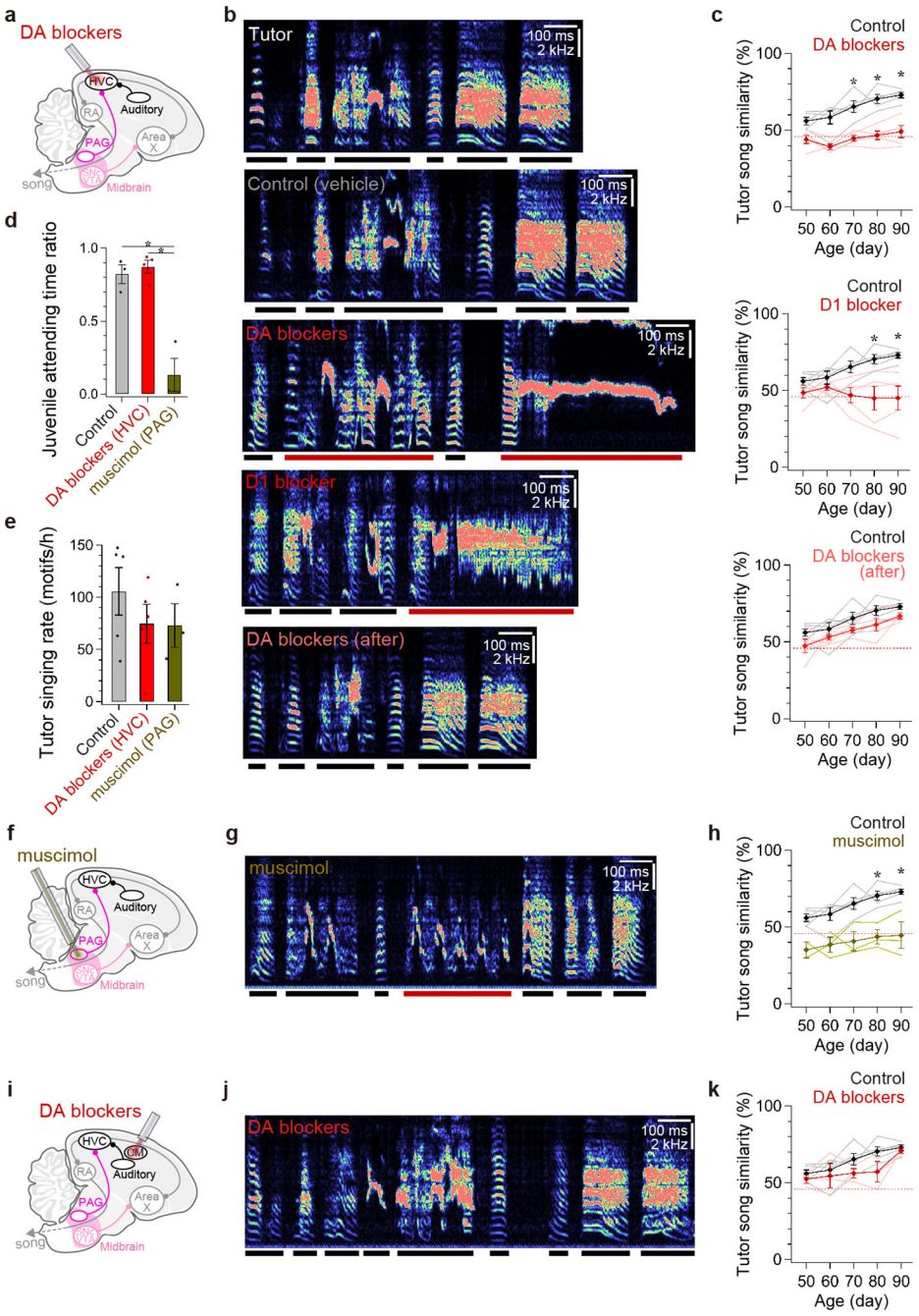

Extended Data Figure 5 |. Effects of infusing DA blockers into HVC or CM and infusing muscimol into PAG on song copying.

a, Schematics showing infusion of DA blockers into HVC. **b**, From top to bottom, sound spectrograms of a song of a tutor bird, a 90-d pupil that received infusion of vehicle during tutoring sessions, a 90-d pupil that received infusion of both D1- and D2-type DA blockers (DA blockers) during tutoring sessions, a 90-d pupil bird that received infusion of D1-type blocker during tutoring sessions, and 90-d pupil that received infusion of both D1- and D2-type DA blockers after tutoring sessions. **c**, Developmental changes in tutor song similarity

of pupils that received infusion of both D1- and D2-type DA blockers (DA blockers) into HVC during tutoring sessions (top, $n = 5$), a D1-type blocker into HVC during tutoring sessions (middle, $n = 5$), or DA blockers into HVC immediately after tutoring sessions (bottom, $n = 5$). Asterisks indicate $P < 0.050$ with Tukey-Kramer test (See Methods). **d**, Proportion of time that juvenile birds attended to the tutor during tutoring sessions was not significantly different between birds that received vehicle ($n = 3$) or DA blockers into HVC ($n = 4$) (Tukey-Kramer test: $P = 0.871$). The attention time of juvenile birds that received infusion of muscimol into PAG ($n = 3$) was lower than that of control birds (Tukey-Kramer test: $P = 0.001$) and that of birds that received injection of DA blockers into HVC (Tukey-Kramer test: $P < 0.001$). **e**, Singing rates of the tutor bird to pupils that received vehicle into HVC ($n = 5$) were not different from that to pupils that received injection of DA blockers into HVC ($n = 5$) or muscimol into PAG ($n = 3$) (one-way ANOVA: $F(2,10) = 0.776$, $P = 0.486$). **f**, Schematics showing infusion of muscimol into PAG. **g**, A sound spectrogram of a song of a 90-d pupil that received infusion of muscimol into PAG during tutoring sessions. A sound spectrogram of the tutor song is shown in **b**. **h**, Tutor song similarity of pupil birds that received infusion of vehicle into HVC and birds that received infusion of muscimol blockers into PAG were significantly different (Tukey-Kramer test: vehicle: $n = 5$, muscimol to PAG: $n = 3$; at 90 d: $P = 0.007$). **i**, Schematics showing infusion of DA blockers into CM (DA blockers possibly diffused into both the medial and lateral CM). **j**, A sound spectrogram of a song of a 90-d pupil that received infusion of DA blockers into CM during tutoring sessions. A sound spectrogram of the tutor song is shown in **b**. **k**, Tutor song similarity of pupil birds that received infusion of vehicle into HVC and birds that received infusion of DA blockers into CM were not significantly different (Tukey-Kramer test: vehicle: $n = 5$, DA blockers to CM: $n = 3$; at 90 d: $P = 1.000$). Horizontal red dashed lines in **c**, **h**, and **k** show song similarity between 90-d untutored birds and unrelated adult male zebra finches that had been raised with normal exposure to a tutor (See Extended Data Fig. 4b-c). Error bars indicate mean ± SEM.

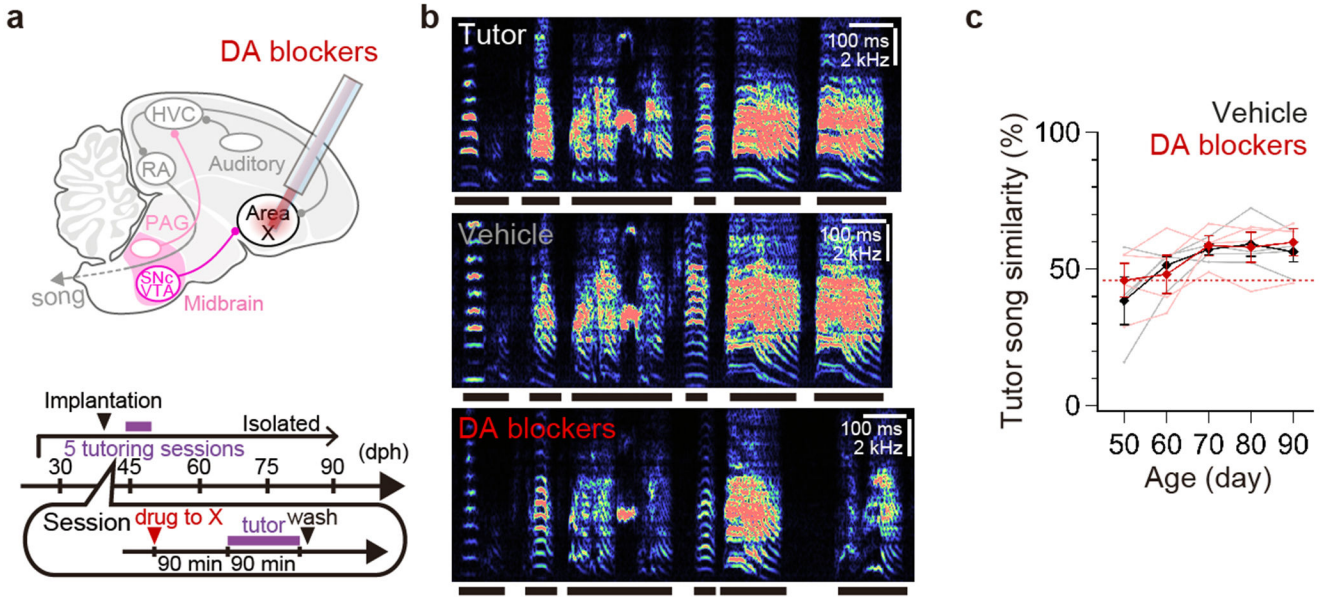

Extended Data Figure 6 |. Infusion of DA blockers into Area X in juvenile males did not disrupt song copying.

a, Schematics (top) and schedule (bottom) of infusion of DA blockers into Area X. **b**, Sound spectrograms of a song of a tutor (top), a 90-d bird that received infusion of vehicle into Area X during tutoring sessions (middle), and a 90-d bird that received infusion of DA blockers into Area X during tutoring sessions (bottom). **c**, Tutor song similarity of pupil birds that received infusion of vehicle into Area X and birds that received infusion of DA blockers into Area X were not significantly different (Tukey-Kramer test: vehicle: $n = 4$, DA blockers: $n = 4$; at 90 d: $P = 1.000$). The horizontal red dashed line shows song similarity between 90-d untutored birds and unrelated adult male zebra finches that had been raised with normal exposure to a tutor (See Extended Data Fig. 4b-c). Error bars indicate mean ± SEM.

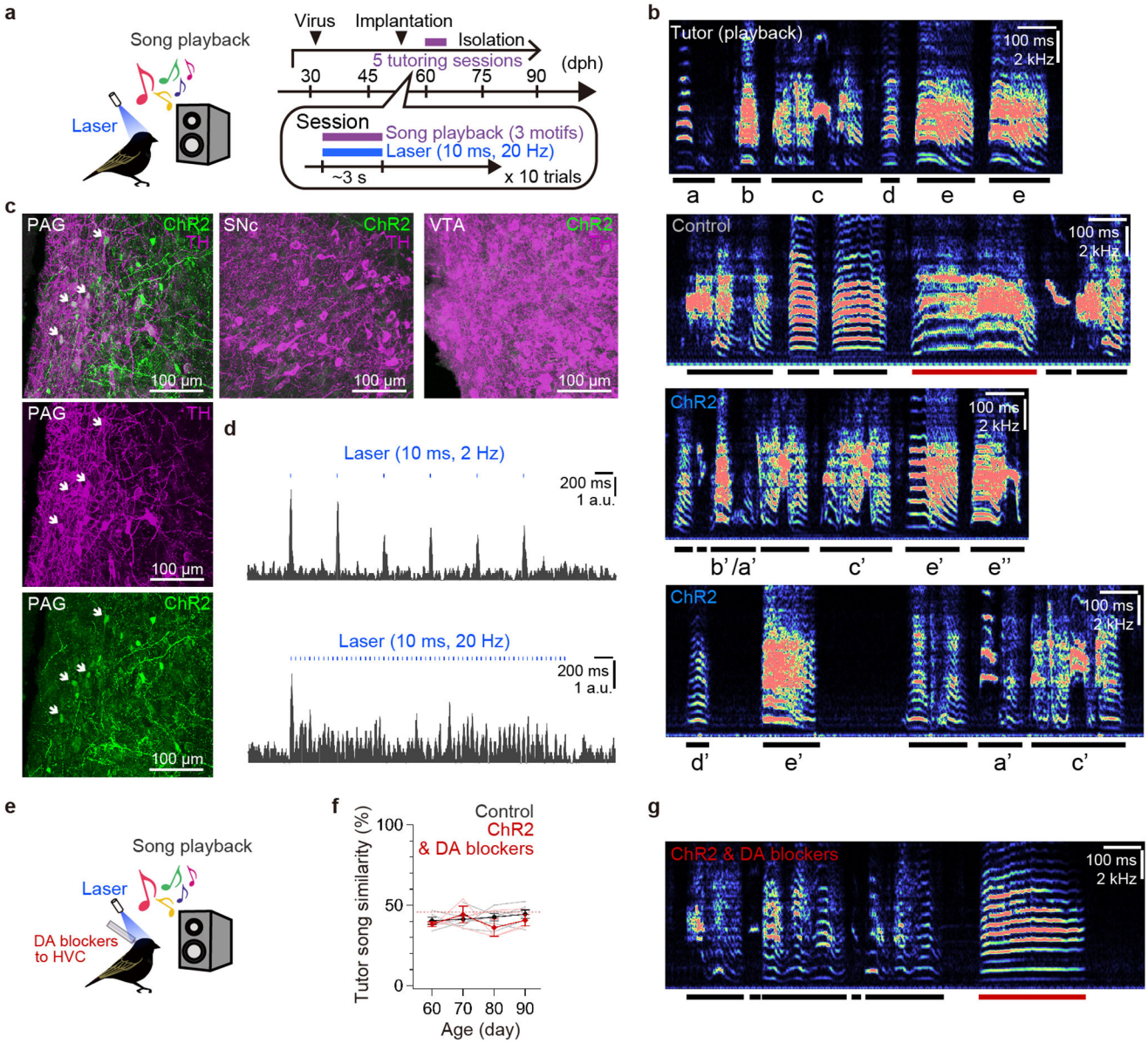

Extended Data Figure 7 |. Optogenetic activation of PAG_{HVC} terminals paired with song playback.

a, Schematics (left) and schedule (right) of optogenetic stimulation of PAG_{HVC} terminals paired with song playback. **b**, Sound spectrograms of song playback used in tutoring sessions (top), a song of a 90-d pupil tutored by song playback without viral injection and laser stimulation (upper middle), and 90-d pupils that received activation of PAG_{HVC} terminals paired with song playback (lower middle and bottom). **c**, From left to right, a max-projected image of serial sagittal sections of PAG (left, ~0.5 mm lateral), showing PAG neurons expressing both ChR2 (green) and TH (pseudo-colored magenta) (arrows), SNc (middle, ~0.8 mm lateral), and VTA (right, ~0.3 mm lateral). Similar results were obtained in 6 independently repeated experiments. **d**, Multiunit activity in PAG, showing time-locked response to laser stimulation at 2 Hz (top) and 20 Hz (bottom). **e**, Schematics of optogenetic stimulation of PAG_{HVC} terminals paired with song playback while infusing DA blockers into HVC. **f**, Tutor song similarity of pupils that received activation of PAG_{HVC} terminals paired with song playback while infusing DA blockers into HVC (red, $n = 3$) was not different from control birds shown in Fig. 3j (Tukey-Kramer test: at 90 d: $P = 1.000$), but lower than that received activation of PAG_{HVC} terminals paired with song playback shown in Fig. 3j (Tukey-Kramer test: at 90 d: $P = 0.019$). **g**, A sound spectrogram of a 90-d pupil that received optogenetic activation of PAG_{HVC} terminals paired with song playback while infusing DA blockers into HVC. A sound spectrogram of the song playback used in tutoring sessions is shown in **b**. Error bars indicate mean ± SEM.

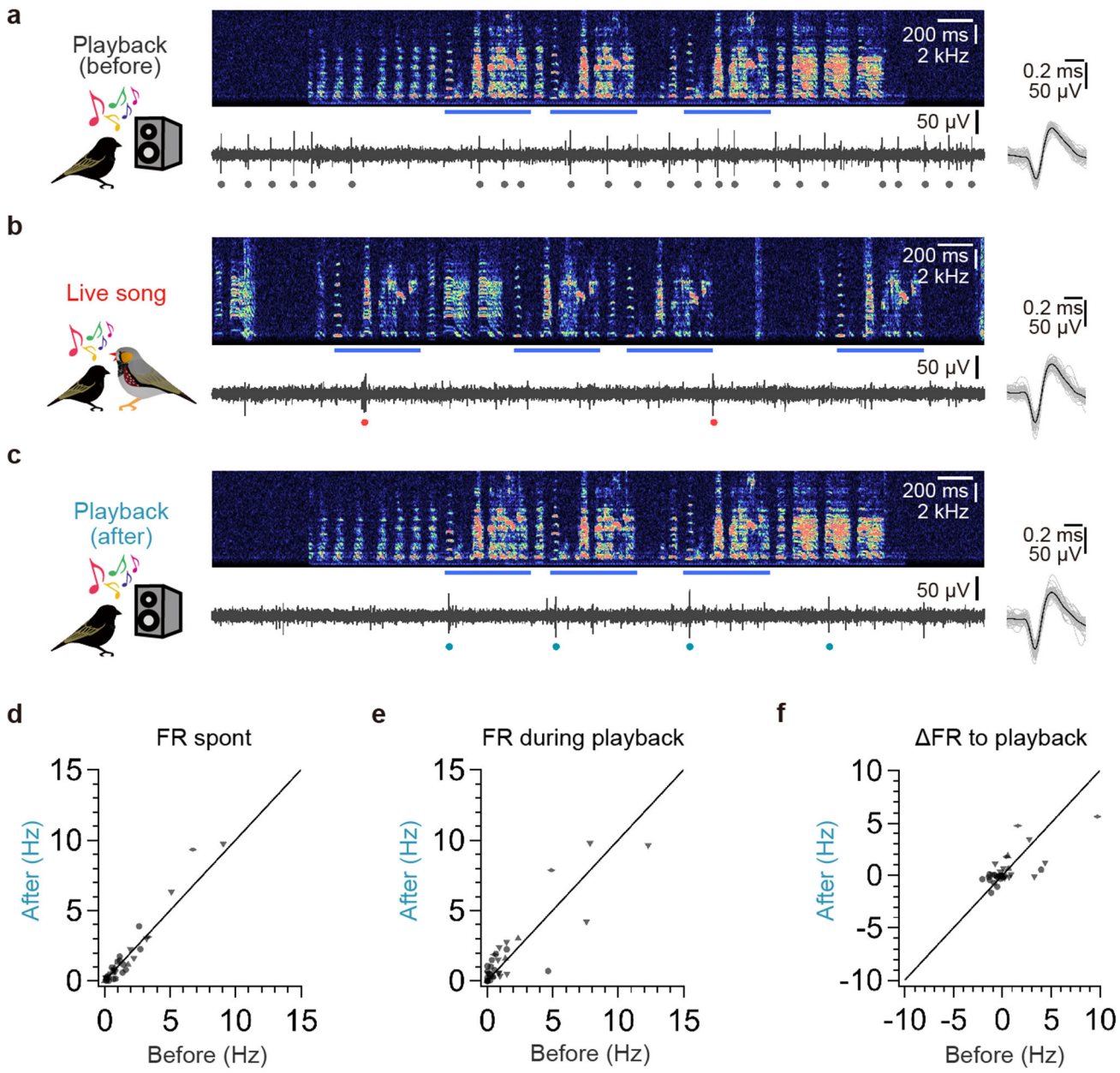

Extended Data Figure 8 |. Spike activity of HVC neurons in juvenile male zebra finches before and after their first exposure to live tutor songs.

a-c, Action potential activity of an HVC neuron to tutor song playback before exposure to a singing tutor (**a**), to live tutor songs (**b**), and to tutor song playback after exposure to live tutor songs (**c**) (top: sound spectrogram, bottom: voltage recording, bottom right: exemplar 50 spikes [gray] and their average [black]. circle: individual spike. blue bar: tutor song motif). **d**, Spontaneous firing rate (FR spont) of HVC neurons of juvenile males before and after exposure to live tutor songs (two-sided paired *t*-test: Mean FR. Before: 1.6 ± 0.3 Hz; After: 1.6 ± 0.4 Hz; $t(34) = 0.794$, $P = 0.433$, $n = 35$, 4 birds). **e**, Firing rate of juvenile male HVC neurons during playback of tutor songs (FR during playback) before and after exposure to live tutor songs (two-sided paired *t*-test: Mean FR. Before: 2.0 ± 0.6 Hz; After:

2.1 ± 0.6 Hz; $t(34) = 0.468$, $P = 0.643$, $n = 35$, 4 birds). **f**, Changes in firing rate (ΔFR) of juvenile HVC neurons in response to playback of tutor songs before and after exposure to live tutor songs (two-sided paired t-test: ΔFR. Before: 0.5 ± 0.4 Hz; After: 0.5 ± 0.2 Hz; $t(34) = 0.079$, $P = 0.937$, $n = 35$, 4 birds).

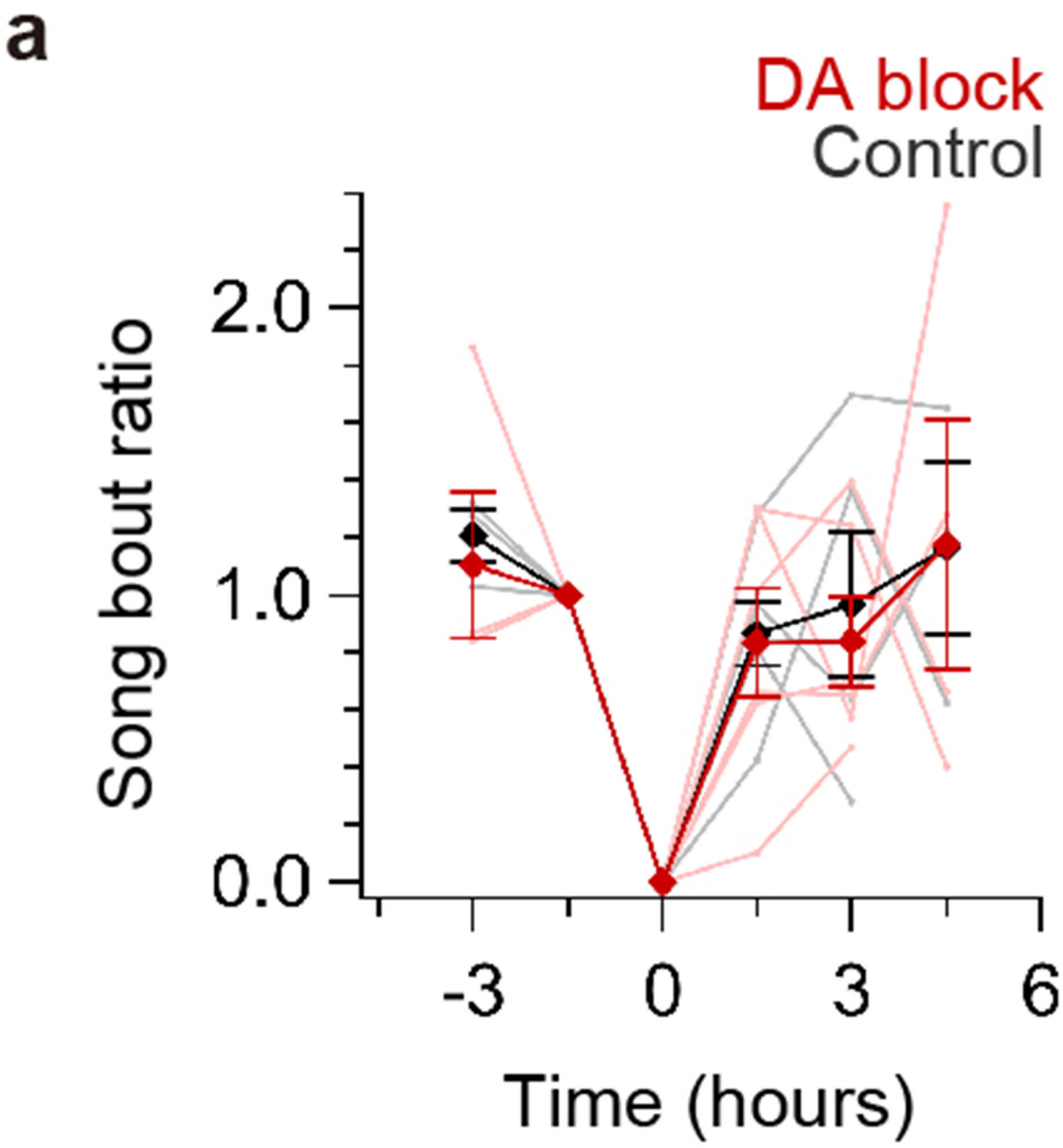

Extended Data Figure 9 |. Song rates of juvenile birds before and after their first tutoring sessions.

a, Ratio of song bouts produced before and after the first tutoring session in control birds (black, $n = 6$) and in birds that received injection of 6-OHDA injections into HVC several

days prior to the tutoring session or that were infused with DA blockers into HVC immediately before and during the tutoring session (red, $n = 6$) . Error bars indicate mean ± SEM.

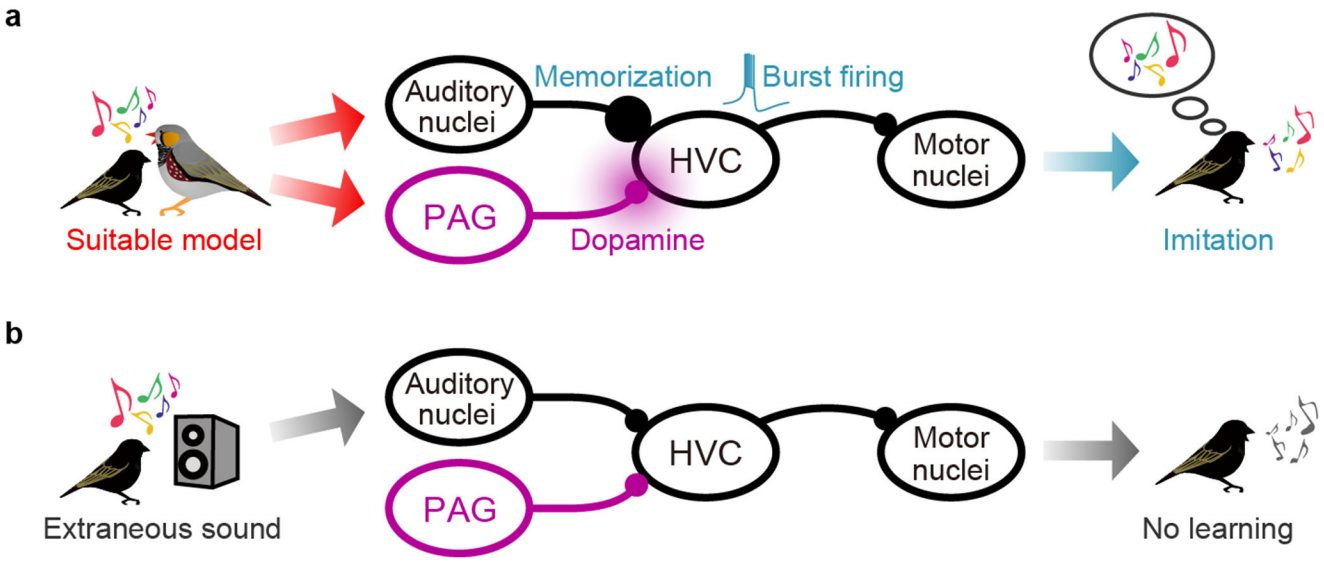

Extended Data Figure 10 |. Summary diagram.

a, The song of a live adult tutor (i.e., a suitable model) activates auditory afferents and DA-releasing PAG afferents to HVC, leading to potentiation and stabilization of auditory synapses in HVC. This plastic change forms temporally precise coding of the tutor songs and increases the occurrence of bursting activity in HVC, which rapidly alters temporal and spectral features of the pupil's vocalization in manner that drives imitation. **b**, Playback of an adult male song without social cues (i.e., extraneous sound) only activates auditory afferents in HVC. The activation of these auditory inputs by itself can neither alter HVC activity nor drive song learning, similar to the condition where DA signaling in the pupil's HVC is blocked during the juvenile's exposure to a live, singing tutor.

Supplementary Material

Refer to Web version on PubMed Central for supplementary material.

Acknowledgements

We thank Jordan Hatfield for constructing AAV2/9-CAG-GRAB$_{DA1h}$. We also thank Stephen Nowicki, Susan Peters, Christopher Sturdy, Fan Wang, and Scott Soderling for critical discussion and for reading earlier versions of this manuscript. This work was supported by JSPS Postdoctoral Fellowship for Research Abroad (M.T.), the National Basic Research Program of China 973 Program Grant 2015CB856402 (Y.L.), the American BRAIN Initiative project 1U01NS103558–01 (Y.L.), NIH Grant 1R01-NS-099288 (R.M.), and NSF IOS-1354962 (R.M.).

References

1. Whiten A Social Learning and Culture in Child and Chimpanzee. Annu Rev Psychol 68, 129–154, doi:10.1146/annurev-psych-010416-044108 (2017). [PubMed: 28051932]

2. Goldstein MH, King AP & West MJ Social interaction shapes babbling: Testing parallels between birdsong and speech. Proceedings of the National Academy of Sciences of the United States of America 100, 8030–8035, doi:10.1073/pnas.1332441100 (2003). [PubMed: 12808137]

3. Marler P & Tamura M Culturally Transmitted Patterns of Vocal Behavior in Sparrows. Science 146, 1483–&, doi:DOI10.1126/science.146.3650.1483 (1964). [PubMed: 14208581]

4. Fehér O, Wang HB, Saar S, Mitra PP & Tchernichovski O De novo establishment of wild-type song culture in the zebra finch. Nature 459, 564–U594, doi:10.1038/nature07994 (2009). [PubMed: 19412161]

5. Chen Y, Matheson LE & Sakata JT Mechanisms underlying the social enhancement of vocal learning in songbirds. Proceedings of the National Academy of Sciences of the United States of America 113, 6641–6646, doi:10.1073/pnas.1522306113 (2016). [PubMed: 27247385]

6. Derégnaucourt S, Poirier C, Kant AV, Linden AV & Gahr M Comparisons of different methods to train a young zebra finch (Taeniopygia guttata) to learn a song. J Physiol Paris 107, 210–218, doi: 10.1016/j.jphysparis.2012.08.003 (2013). [PubMed: 22982543]

7. Aronov D, Andalman AS & Fee MS A specialized forebrain circuit for vocal babbling in the juvenile songbird. Science 320, 630–634, doi:10.1126/science.1155140 (2008). [PubMed: 18451295]

8. Derégnaucourt S, Mitra PP, Feher O, Pytte C & Tchernichovski O How sleep affects the developmental learning of bird song. Nature 433, 710–716, doi:10.1038/nature03275 (2005). [PubMed: 15716944]

9. Nottebohm F, Stokes TM & Leonard CM Central Control of Song in Canary, Serinus-Canarius. J Comp Neurol 165, 457–486, doi:DOI10.1002/cne.901650405 (1976). [PubMed: 1262540]

10. Roberts TF, Gobes SM, Murugan M, Olveczky BP & Mooney R Motor circuits are required to encode a sensory model for imitative learning. Nat Neurosci 15, 1454–1459, doi:10.1038/nn.3206 (2012). [PubMed: 22983208]

11. Fortune ES & Margoliash D Parallel Pathways and Convergence onto Hvc and Adjacent Neostriatum of Adult Zebra Finches (Taeniopygia-Guttata). J Comp Neurol 360, 413–441, doi:DOI10.1002/cne.903600305 (1995). [PubMed: 8543649]

12. Coleman MJ & Mooney R Synaptic transformations underlying highly selective auditory representations of learned birdsong. J Neurosci 24, 7251–7265, doi:10.1523/JNEUROSCI. 0947-04.2004 (2004). [PubMed: 15317851]

13. Appeltants D, Absil P, Balthazart J & Ball GF Identification of the origin of catecholaminergic inputs to HVc in canaries by retrograde tract tracing combined with tyrosine hydroxylase immunocytochemistry. J Chem Neuroanat 18, 117–133 (2000). [PubMed: 10720795]

14. Hamaguchi K & Mooney R Recurrent interactions between the input and output of a songbird cortico-basal ganglia pathway are implicated in vocal sequence variability. J Neurosci 32, 11671–11687, doi:10.1523/JNEUROSCI.1666-12.2012 (2012). [PubMed: 22915110]

15. Kingsbury MA, Kelly AM, Schrock SE & Goodson JL Mammal-like organization of the avian midbrain central gray and a reappraisal of the intercollicular nucleus. PLoS One 6, e20720, doi: 10.1371/journal.pone.0020720 (2011). [PubMed: 21694758]

16. Cho JR et al. Dorsal Raphe Dopamine Neurons Modulate Arousal and Promote Wakefulness by Salient Stimuli. Neuron 94, 1205–1219 e1208, doi:10.1016/j.neuron.2017.05.020 (2017). [PubMed: 28602690]

17. Matthews GA et al. Dorsal Raphe Dopamine Neurons Represent the Experience of Social Isolation. Cell 164, 617–631, doi:10.1016/j.cell.2015.12.040 (2016). [PubMed: 26871628]

18. Flores JA, Galan-Rodriguez B, Ramiro-Fuentes S & Fernandez-Espejo E Role for dopamine neurons of the rostral linear nucleus and periaqueductal gray in the rewarding and sensitizing properties of heroin. Neuropsychopharmacol 31, 1475–1488, doi:10.1038/sj.npp.1300946 (2006).

19. Sun F, Zeng J, Jing M Zhou J, Feng J, Owen SF, Luo Y, Li F, Wang H, Yamaguchi T, Yong Z, Gao Y, Peng W, Wang L, Zhang S, Du J, Lin D, Xu M, Kreitzer AC, Cui G & Li Y A Genetically Encoded Fluorescent Sensor Enables Rapid and Specific Detection of Dopamine in Flies, Fish, and Mice. Cell 174, 481–496, doi:10.1016/j.cell.2018.06.042 (2018). [PubMed: 30007419]

20. Roberts TF, Tschida KA, Klein ME & Mooney R Rapid spine stabilization and synaptic enhancement at the onset of behavioural learning. Nature 463, 948–952, doi:10.1038/nature08759 (2010). [PubMed: 20164928]
21. Ungerstedt U & Arbuthnott GW Quantitative recording of rotational behavior in rats after 6-hydroxy-dopamine lesions of the nigrostriatal dopamine system. Brain Res 24, 485–493 (1970). [PubMed: 5494536]
22. Eales LA Song Learning in Zebra Finches - Some Effects of Song Model Availability on What Is Learnt and When. Animal Behaviour 33, 1293–1300, doi:Doi10.1016/S0003-3472(85)80189-5 (1985).
23. Tanaka M, Singh Alvarado J, Murugan M & Mooney R Focal expression of mutant huntingtin in the songbird basal ganglia disrupts cortico-basal ganglia networks and vocal sequences. Proceedings of the National Academy of Sciences of the United States of America 113, E1720–1727, doi:10.1073/pnas.1523754113 (2016). [PubMed: 26951661]
24. Kubikova L, Wada K & Jarvis ED Dopamine receptors in a songbird brain. J Comp Neurol 518, 741–769, doi:10.1002/cne.22255 (2010). [PubMed: 20058221]
25. Hisey E, Kearney MG & Mooney R A common neural circuit mechanism for internally guided and externally reinforced forms of motor learning. Nat Neurosci, doi:10.1038/s41593-018-0092-6 (2018).
26. Roberts TF et al. Identification of a motor-to-auditory pathway important for vocal learning. Nat Neurosci 20, 978–986, doi:10.1038/nn.4563 (2017). [PubMed: 28504672]
27. London SE & Clayton DF Functional identification of sensory mechanisms required for developmental song learning. Nat Neurosci 11, 579–586, doi:10.1038/nn.2103 (2008). [PubMed: 18391944]
28. Bao S, Chan VT & Merzenich MM Cortical remodelling induced by activity of ventral tegmental dopamine neurons. Nature 412, 79–83, doi:10.1038/35083586 (2001). [PubMed: 11452310]
29. Berger B, Gaspar P & Verney C Dopaminergic innervation of the cerebral cortex: unexpected differences between rodents and primates. Trends Neurosci 14, 21–27 (1991). [PubMed: 1709528]
30. Williams SM & Goldman-Rakic PS Widespread origin of the primate mesofrontal dopamine system. Cereb Cortex 8, 321–345 (1998). [PubMed: 9651129]

Method references

31. Tchernichovski O, Nottebohm F, Ho CE, Pesaran B & Mitra PP A procedure for an automated measurement of song similarity. Anim Behav 59, 1167–1176, doi:10.1006/anbe.1999.1416 (2000). [PubMed: 10877896]

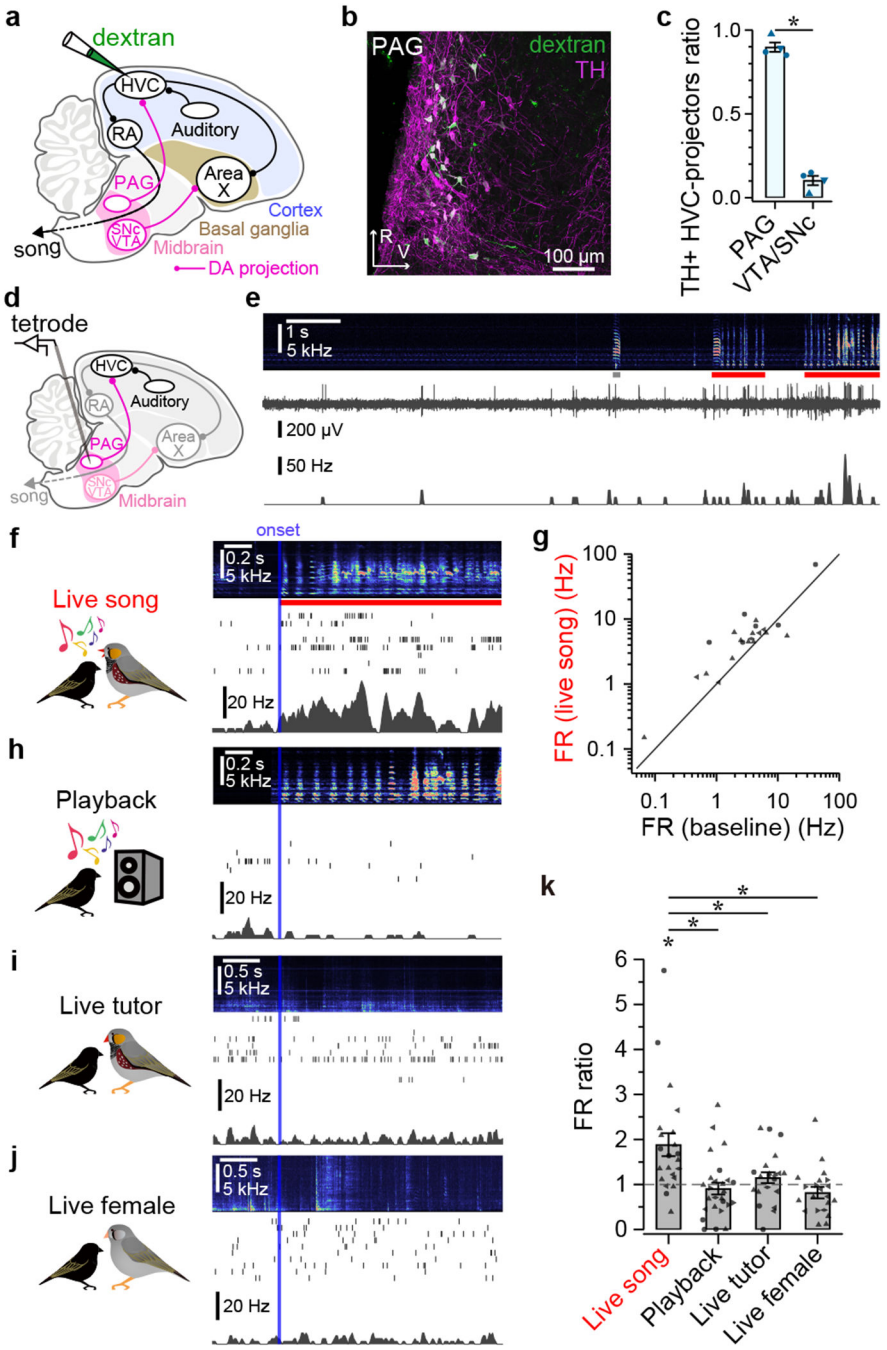

Figure 1 |. Recordings of PAG activity.

a, Schematics of dextran injection into HVC. **b**, PAG neurons labeled with dextran (green) and TH antibody (pseudo-colored magenta) (~0.5 mm lateral, R: rostral, V: ventral). **c**, Proportion of double-labeled neurons (dextran and TH) in the midbrain (χ^2-test: $\chi^2(1) = 623.02$, $P < 0.001$, $n = 4$ hemispheres from 3 birds). **d**, Schematics of tetrode recordings from PAG neurons. **e**, PAG unit activity during live tutor songs (red bar) (gray bar: an isolated tutor call) (top: sound spectrogram, middle: voltage recording, bottom: firing rate). **f**, PAG unit activity aligned to the onset of tutor songs (top: averaged spectrogram, middle:

spike raster, bottom: mean firing rate). **g**, Mean firing rate (FR) during live tutor songs as a function of baseline FR of PAG neurons. **h-j**, PAG unit activity aligned to the onset of song playback (**h**), encounters with a live, non-singing tutor (**i**), encounters with a live female (**j**), shown as in **f**. **k**, Mean FR of PAG neurons normalized to baseline FR (two-sided paired *t*-test: Live song: $t(21) = 3.439$, $P = 0.002$; Playback: $t(25) = 0.278$, $P = 0.783$; Live tutor: $t(21) = 1.270$, $P = 0.218$; Live female: $t(19) = 1.339$, $P = 0.196$; $n = 26$ neurons, 5 birds). Error bars indicate mean ± SEM.

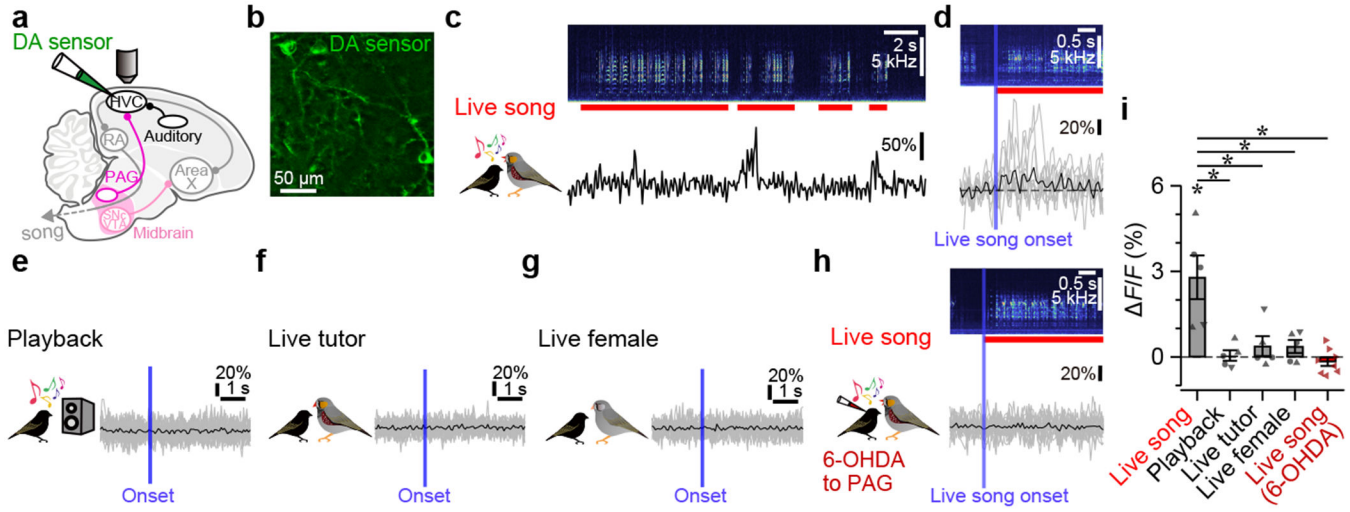

Figure 2 |. Imaging of DA in HVC.

a, Schematics of two-photon imaging of DA sensors ($GRAB_{DA1h}$) in HVC. **b**, Two-photon image of HVC neurons expressing DA sensors. **c**, Fluorescence changes ($\Delta F/F$) of $GRAB_{DA1h}$ in a juvenile's HVC neuron in response to live tutor songs (red bars) **d**, $\Delta F/F$ aligned to the onset of live tutor songs (gray: individual, black: mean). **e-h**, $\Delta F/F$ aligned to the onset of song playback (**e**), encounters with a live, non-singing tutor (**f**), encounters with a live female (**g**), and live tutor songs after 6-OHDA injection into PAG (**h**). **i**, Mean $\Delta F/F$ of HVC neurons (two-sided paired *t*-test: Live song: $t(4) = 3.660$, $P = 0.022$; Playback: $t(4) = 0.261$, $P = 0.807$; Live tutor: $t(4) = 1.092$, $P = 0.336$; Live female: $t(4) = 1.589$, $P = 0.187$; Live song after 6-OHDA injection into PAG: $t(7) = 1.122$, $P = 0.324$; $n = 13$ neurons, 5 birds). Error bars indicate mean ± SEM.

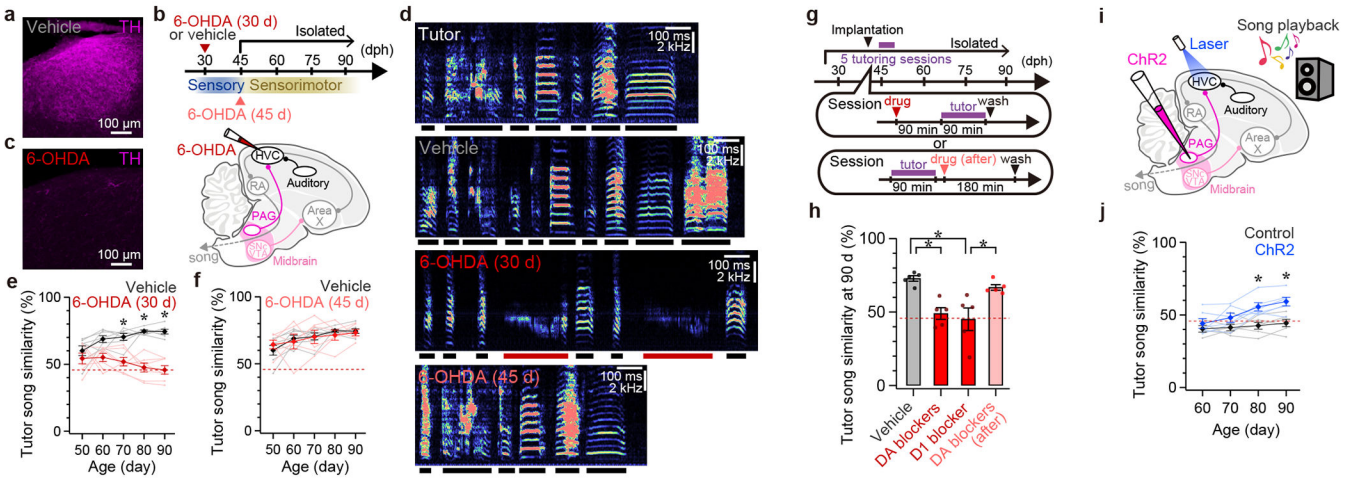

Figure 3 |. Chemical blockade and optogenetic activation of DA signaling in HVC.

a, DA fibers in HVC (pseudo-colored magenta: TH) (~2.4 mm lateral). **b**, Timeline and schematics of 6-OHDA injection into HVC. **c**, Loss of DA fibers in HVC after 6-OHDA injection at 29 d, as in **a** (~2.4 mm lateral). **d**, From top to bottom, spectrograms of a song from the tutor bird and songs from 90-d pupil birds that received injection into HVC of vehicle, 6-OHDA at ~30 d, or 6-OHDA at ~45 d (red bars denote abnormally long syllables. See Extended Data Fig. 4b-c). **e**, Absence of song copying following injection of 6-OHDA into HVC at ~30 d (Tukey-Kramer test: vehicle: $n = 7$, 6-OHDA: $n = 7$; at 90 d: $P < 0.001$). **f**, Normal levels of song copying were achieved following injection of 6-OHDA into HVC at ~45 d (Tukey-Kramer test: vehicle: $n = 7$ [same birds as in **e**], 6-OHDA at 45 d: $n = 6$; at 90 d: $P = 1.000$). **g**, Timeline of DA blocker infusion into HVC using microdialysis. **h**, Tutor song similarity of 90-d pupils that received infusion into HVC of vehicle during tutoring ($n = 5$), DA blockers during tutoring (Tukey-Kramer test: vs. vehicle: $P = 0.011$, $n = 5$), D1-type blocker during tutoring (Tukey-Kramer test: vs. vehicle: $P < 0.001$, $n = 5$), or DA blockers after tutoring (Tukey-Kramer test: vs. vehicle: $P = 1.000$; $n = 5$). **i**, Schematics of PAG_{HVC} terminal activation paired with song playback. **j**, Song copying is facilitated by pairing playback with PAG_{HVC} terminal activation in tutor-naive juveniles (Tukey-Kramer test: ChR2: $n = 6$; control: $n = 6$; at 90 d: $P = 0.023$). Horizontal red dashed lines in **e**, **f**, **h**, and **j** show song similarity between 90-d untutored birds to unrelated adults (See Extended Data Fig. 4b-c). Error bars indicate mean ± SEM.

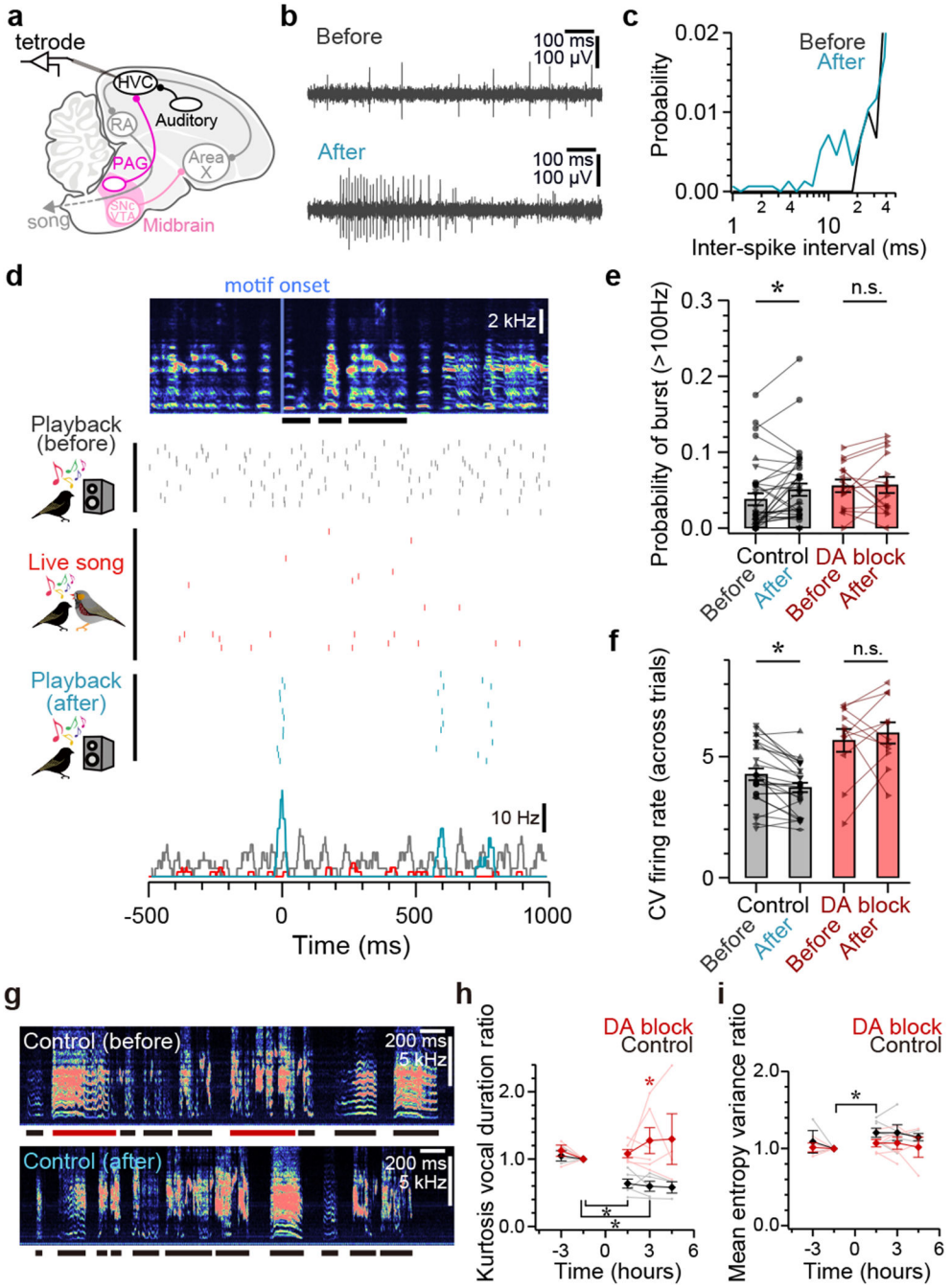

Figure 4 |. Changes in HVC activity and song features after live tutoring.

a, Schematic of HVC recordings in pupils. **b-c**, Spontaneous HVC unit activity (**b**) and the histogram of the interspike intervals before (black) and after (cyan) live tutoring (**c**). **d**, HVC unit activity aligned to tutor song motif onset (top: averaged spectrogram; middle: raster, bottom: mean FR across trials; horizontal bars: syllables). **e**, Probability of burst activity (>100 Hz) increased after live tutoring in control juveniles (two-sided paired *t*-test: $t(34) = 2.490$, $P = 0.018$, $n = 35$ neurons, 4 birds), but not in juveniles with 6-OHDA injected into HVC (two-sided paired *t*-test: $t(13) = 0.774$, $P = 0.453$, $n = 14$ neurons, 2 birds). **f**,

Coefficients of variance (CV) of firing rate across trials increased in control juveniles (two-sided paired *t*-test: $t(25) = 4.080$, $P < 0.001$, $n = 26$ neurons, 4 birds), but not in juveniles with 6-OHDA injected into HVC (two-sided paired *t*-test: $t(10) = 0.640$, $P = 0.537$, $n = 11$ neurons, 2 birds). **g**, Spectrograms of juvenile songs before (top) and after (bottom) live tutoring (red bar: long vocalization). **h**, After live tutoring, kurtosis of vocal duration decreased in control juveniles (two-sided paired *t*-test: 1.5 h: $t(5) = 5.563$, Bonferroni corrected $P = 0.008$, $n = 6$), but not in juveniles with 6-OHDA or DA blockers injected into HVC (two-sided paired *t*-test: 1.5 h: $t(5) = 1.364$, Bonferroni corrected $P = 0.692$, $n = 6$). **i**, After live tutoring, mean Wiener entropy variance (EV) increased in control juveniles (two-sided paired *t*-test: at 1.5 h: $t(5) = 4.059$, Bonferroni corrected $P = 0.029$, $n = 6$), but not in juveniles with 6-OHDA or DA blockers injected into HVC (two-sided paired *t*-test: at 1.5 h: $t(5) = 1.432$, Bonferroni corrected $P = 0.635$, $n = 6$). Juveniles did not sing during tutoring (0–1.5 h. See Extended Data Fig. 9). Error bars indicate mean ± SEM.